Journal of Power Sources 196 (2011) 1474–1477

Contents lists available at ScienceDirect

Journal of Power Sources

journal homepage: www.elsevier.com/locate/jpowsour

Short communication

Whisker formation on a thin film tin lithium-ion battery anode

Juchuan Li[a,*], Fuqian Yang[a], Jia Ye[b], Yang-Tse Cheng[a]

[a] Department of Chemical and Materials Engineering, University of Kentucky, 177 F Paul Anderson Tower, Lexington, KY 40506, USA
[b] Electron Microscopy Center, University of Kentucky, Lexington, KY 40506, USA

ARTICLE INFO

Article history:
Received 30 July 2010
Received in revised form 29 August 2010
Accepted 31 August 2010
Available online 8 September 2010

Keywords:
Anode (negative electrode)
Lithium-ion battery
Sn (tin)
Sn whisker (tin whisker)

ABSTRACT

Tin (Sn) is a candidate material for anodes (negative electrodes) of lithium-ion batteries because of its high theoretical energy capacity. In this paper, we report an observation of Sn-whisker growth on Sn-thin films after lithiation and delithiation. The compressive stress generated by electrochemical lithiation of the Sn-thin films is likely the driving force for the growth of the Sn whiskers. Attention should therefore be paid to the issue of Sn-whisker growth for Sn-based electrodes since Sn whiskers may penetrate through the separator, and short-circuit the electrochemical cell.

1. Introduction

Li-ion batteries (LIBs) are widely used as power supplies for various electronic devices due to their high energy and power densities. The growing demands for electronic devices, portable tools, and hybrid and all-electric vehicles require batteries with higher capacity and longer durability. Commercial graphite anodes used in LIBs have good cycling behavior with a capacity of 372 mAh g^{-1} [1]. Sn is one of the prominent materials for the negative electrodes of LIBs because of its high gravitational and volumetric capacities (992 mAh g^{-1} and 7262 mAh cm^{-3}, respectively [2]). However, the volume change from pure Sn to its fully lithiated phase ($Li_{4.4}Sn$) is approximately 260% [3]. This large volume change results in fracture and pulverization of the active material and poor cycling ability, which hinders its application as an electrode material. The large stress and strain created by volume expansion and contraction are the cause of cracks and fracture of the active materials [4–6].

The electrochemical performance of Sn-based alloys, such as Sn–Cu [7–9], Sn–Ni [9,10], Sn–Zn [11], and Sn–Co [12,13], has been studied. Capacity retention is improved due to the formation of active/inactive structure in these Sn alloys. The cycling performance of materials can also be enhanced by using nano-scale structures [14–16].

Furthermore, safety is a key issue for LIBs. But, there are few reports on the safety studies of Sn-based electrodes. In this work, we report the first observation of Sn-whisker formation after lithiation and delithiation. The Sn whiskers may be a safety concern for Sn-based LIBs.

2. Experimental

Sn-thin films were deposited on 0.5 mm thick stainless steel discs by radio frequency (RF) magnetron sputtering using an Advanced Energy system. A pure Sn target (99.998%, Kurt J. Lesker) of 25.4 mm diameter was used in the sputtering. Pre-sputtering was carried out in ultra-high-purity Ar (99.999%, Scott-Gross) at 50 W for 5 min to remove any oxides and contaminations on the Sn target surface. Sn sputtering was performed in argon with a working pressure of 3 Pa and a power of 30 W. The substrate was kept at room temperature of about 23 °C during sputtering. The film thickness was recorded by a quartz crystal microbalance thickness monitor (Inficon) during sputtering, and was examined by a Dektak 3030 profilometer (Veeco) after sputtering. Immediately after sputtering, samples were annealed at 200 °C under Ar atmosphere for 2 h to remove internal stresses generated during the sputtering.

The electrochemical performance of the as-prepared Sn-thin films was evaluated using 2025-type coin cells (Hohsen). The stainless steel substrate served as the current collector to obtain a uniform current distribution. Pure lithium foils (99.9%, Sigma–Aldrich) were cut into proper size and used as the counter electrode. Poly-propylene woven separators (Celgard 3501) were used in the coin cells. 1 M $LiPF_6$ in ethylene carbonate/dimethyl carbonate (EC/DMC, 1:1 by vol.) was used as the electrolyte (Novolyte). Electrochemical performance was conducted using a VMP3 multichannel potentiostat/galvanostat (Bio-Logic). Galvanostatic cycling of the cells was carried out at a rate of C/10 between 1.2 V and 0.02 V.

* Corresponding author. Tel.: +1 8592186530; fax: +1 8593231929.
E-mail address: jlin@engr.uky.edu (J. Li).

0378-7753/$ – see front matter © 2010 Elsevier B.V. All rights reserved.
doi:10.1016/j.jpowsour.2010.08.116

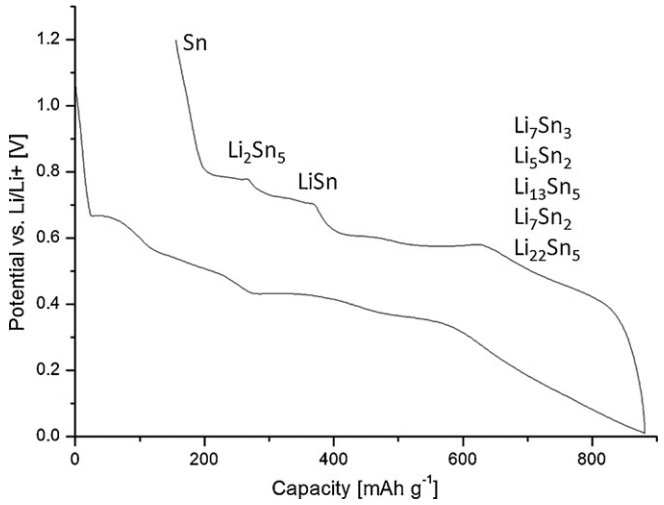

Fig. 1. First cycle galvanostatic discharge/charge curve of Sn at C/10. The reversible capacity of Sn is 725 mAh g^{-1} (corresponding to 3.2 Li atoms per Sn atom), and the irreversible capacity is 155 mAh g^{-1}.

After cell disassembly, the Sn-thin films were cleaned using DMC (99%, Alfa Aesar), and then examined by scanning electron microscope (SEM, Hitachi S-4300 at 3 kV) and field emission transmission electron microscope (FETEM, JEOL 2010F at 200 kV).

3. Results and discussion

Before performing the first galvanostatic cycle, the Sn electrode was rapidly lithiated to 1.2 V relative to pure Li to avoid the anomalous irreversible capacity during initial lithiation of Sn [17]. The initial galvanostatic cycle within the 0.02–1.2 V potential window is shown in Fig. 1. The Sn-thin film electrode had a reversible capacity of 725 mAh g^{-1} during the first cycle. The irreversible capacity of 155 mAh g^{-1} at the first cycle was mainly due to the formation of solid electrolyte interphase (SEI) on the electrode, which consumed Li ions from the electrolyte [18]. After removing the effect of SEI on the initial lithiation capacity, the calculated Li to Sn atomic ratio is 3.2:1. This ratio suggests a combination of Li–Sn phases which do not have a long-range ordered structure [19]. The theoretical capacity of Sn (992 mAh g^{-1}) is calculated based on the formation of the ultimate phase of lithiation, $Li_{4.4}Sn$. However, it is difficult for Sn to be fully lithiated to the state of 4.4 Li atoms per Sn atom at room temperature, due to the limited diffusivity of Li atoms in Sn and Li_xSn_y phases, and due to the non-equilibrium electrochemical condition. Our results of Sn cycling show that even at a relatively slow rate of C/70, $Li_{3.8}Sn$ formed after full lithiation. This observation is consistent with a previous study [19].

To compare the structural change of Sn-thin films due to the electrochemical cycling, the morphology of 500 nm Sn films before and after electrochemical lithiation, and after delithiation is shown in Fig. 2. During sputtering, Sn-thin films were not uniform due to the high mobility of Sn atoms. Though the surface of the as-prepared Sn-thin film was not uniform, there was no whisker growth observed after the sputtering. Furthermore, no whisker formation was observed after leaving the Sn-thin films in ambient environment for 30 days. This indicates that the internal stress was negligible in the Sn-thin films after annealing. However, after lithiation, the formation of long Sn whiskers and large Sn hillocks was observed, as shown in Fig. 2(b). The average number of Sn whiskers per unit area was calculated to be 1306 ± 280 in 1 mm^2. The length of the Sn whiskers ranges from several μm to 30 μm, with a diameter of 150–300 nm. In addition, cracks formed on Sn-thin films after the first lithiation/delithiation cycle, as shown in Fig. 2(c).

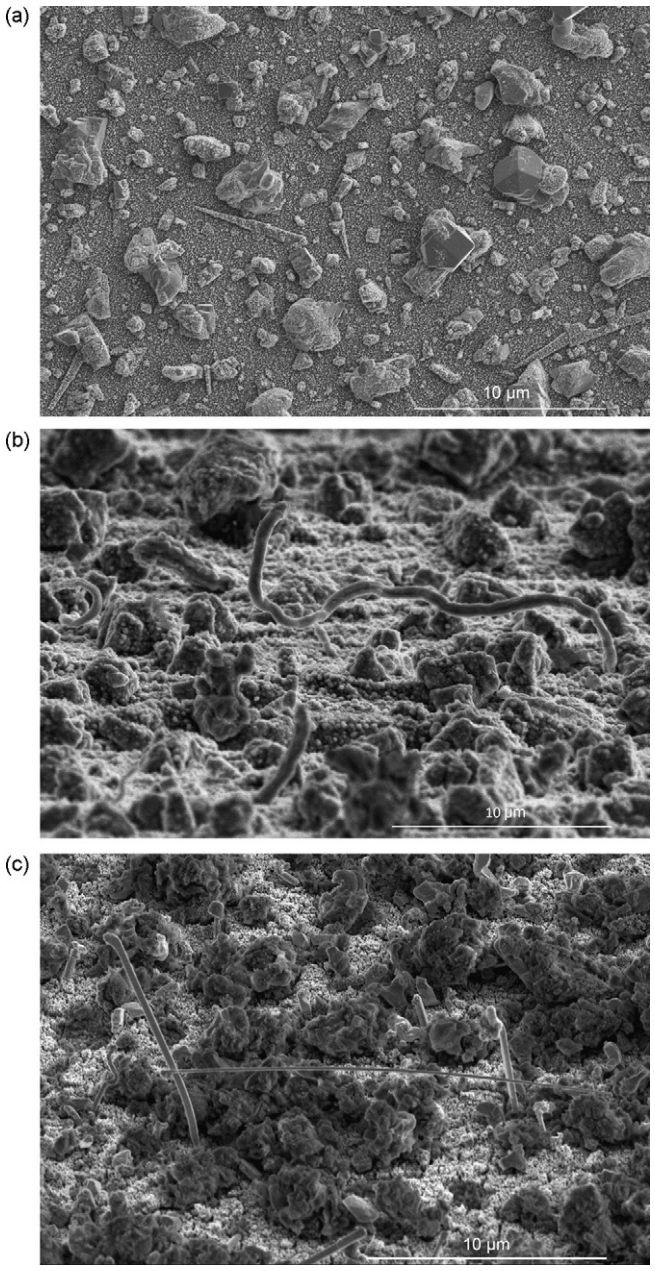

Fig. 2. (a) A SEM image of Sn after annealing at 200 °C for 2 h. (b) Surface morphology of Sn at the stage of full lithiation. The sample stage is tilted at 80°. (c) Surface morphology of Sn after one cycle of Li insertion/extraction. The sample stage is tilted at 60°.

Fig. 3(a) and (b) shows the FETEM image of a randomly selected whisker after one cycle of lithiation/delithiation. The sharp edges and corners of the whisker in Fig. 3(a) and the periodic atomic structure in Fig. 3(b) indicate that the whisker is a single crystal, whose crystal structure was confirmed by selected area electron diffraction (SAED, inset of Fig. 3(a)) to be body-centered tetragonal (β-Sn) with the [0 1 −2] direction along the axis of the whisker. There is an amorphous layer covering the crystalline whisker, which may be the remaining SEI layer [20] after sample cleaning by DMC or an oxide layer [21,22] formed during the TEM sample preparation. While the majority of the layer is amorphous, a small portion shows aligned structure, suggesting crystallization of SEI as indicated by the circle in Fig. 3(b).

Sn-whisker formation and growth have been extensively studied, and Sn whiskers have been observed on electrodeposited and

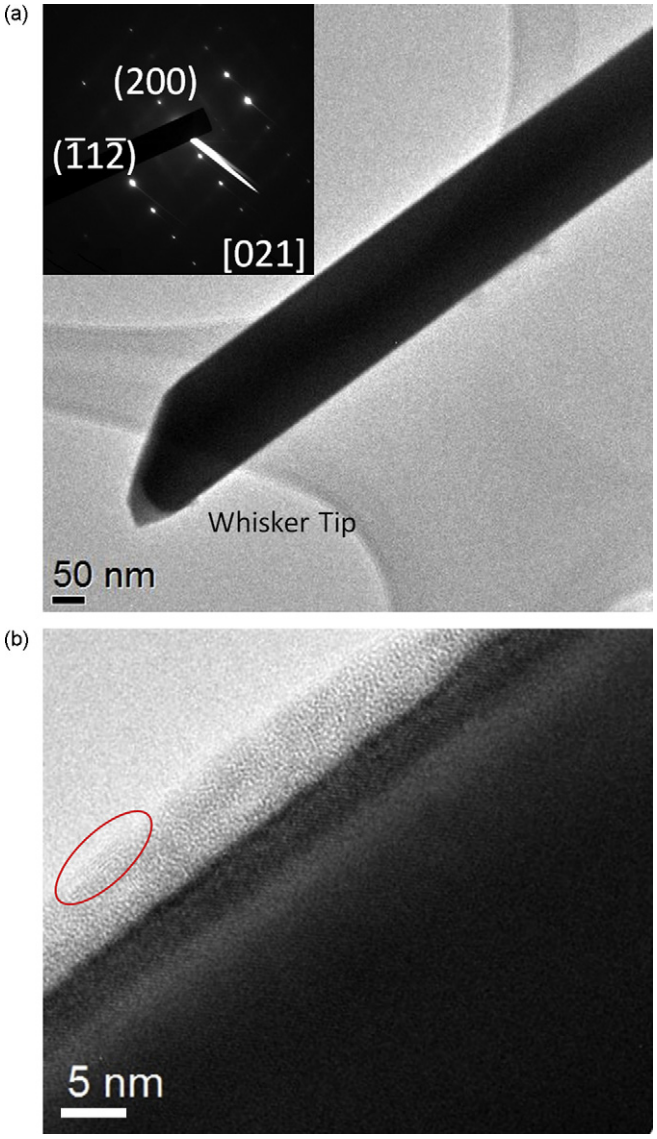

Fig. 3. (a) A TEM image of a randomly selected Sn whisker after discharging/charging for one cycle. The inset SAED indicates single crystal whisker with growth direction of [0 1 −2]. (b) Enlargement of the whisker in (a). The circle indicates aligned structure of the amorphous shell on the crystalline whisker.

sputtered Sn-thin films [23–25]. Sn whiskers usually form due to stresses which are generated during solid-state reaction of Sn and the Cu substrate to form intermetallic compounds, such as Cu_6Sn_5 [25–27]. Generally, whisker growth is a result of the compressive stress along the thickness direction of the film by a "squeeze out" mechanism [25,28]. A related phenomenon is the stress-induced growth of nanowires caused by hundreds of MPa of compressive stress incurred during film deposition [29]. Recently, the effect of aging time on Sn-whisker growth from thin films and their anode behaviors in LIBs have been studied [30].

In the present experiment, intermetallics do not form between the Sn-thin film and the stainless steel substrate. The formation of Sn whiskers is likely caused by the lithiation-induced stress. During lithiation, Li and Sn form Li_xSn phases, which create large compressive stress in the Sn film because of volume expansion and constrain of the substrate. Our results of stress measurement using a home-built laser-curvature device show that the compressive stress in Sn-thin films is about 700 MPa during lithiation. This compressive stress, which is higher than what is usually required for Sn-whisker growth, leads to the "squeeze out" of Sn atoms form Sn whiskers during lithiation.

Pure Li metal has several advantages over other anode materials for LIBs, including large specific capacity, and high energy density. However, a detrimental phenomenon that impedes the application of pure Li metal as anodes of LIBs is the morphological change of Li metal and the formation of Li dendrites [31–33] during electrochemical cycling. The Li dendrites can penetrate through the separator, short-circuit the electrochemical cell, and thus causes serious safety problems. Safety is more prominent in the application of large number of cells, such as hybrid and all-electric vehicles, than individual cells, since the probability of failure of a battery pack consisting of many individual battery cells in series is proportional to the number of cells. Problems with any individual cell could damage the whole power supply.

The shear moduli of pure Sn and pure Li at room temperature are 19.0 GPa [34] and 4.2 GPa [35], respectively. It is expected that the strength of single crystal Sn whiskers is much greater than single crystal and polycrystalline Li dendrites, because the theoretical strength of a single crystal is approximately 1/10 of its shear modulus. Similar to the lithium dendrites, Sn whiskers may also penetrate through the porous polymer separator and cause a short-circuit of the LIB. Actually, the initial interest in study on Sn whiskers was raised by the fact that Sn whiskers formed from solders could short-circuit electronic circuits and destroy electronic devices. The observed formation of Sn whiskers during lithiation of Sn-thin film electrodes suggests the need for more detailed studies of whisker formation in alloy electrodes consisting of low melting point elements, such as Sn, as well as the effects of whiskers on the safely of LIBs.

4. Conclusions

We report the first observation of Sn-whisker growth after lithiation of Sn-thin film electrodes. The formed whiskers are pure Sn single crystal. The high compressive stress during lithiation is likely the driving force for the whisker growth. Since these whiskers may short-circuit the cells, more detailed studies of lithiation-induced whisker growth and their safety implications are needed for Sn-based electrodes in LIB applications.

Acknowledgements

The financial support from NSF (CMMI #1000726) and General Motors Global R&D Center is greatly acknowledged. FY is grateful to the Kentucky Science and Engineering Foundation for financial support through grant agreement KSEF-148-502-06-180.

References

[1] J.R. Dahn, T. Zheng, Y.H. Liu, J.S. Xue, Science 270 (1995) 590–593.
[2] D. Larcher, S. Beattie, M. Morcrette, K. Edstroem, J.C. Jumas, J.M. Tarascon, Journal of Materials Chemistry 17 (2007) 3759–3772.
[3] L.Y. Beaulieu, K.W. Eberman, R.L. Turner, L.J. Krause, J.R. Dahn, Electrochemical and Solid State Letters 4 (2001) A137–A140.
[4] Y.T. Cheng, M.W. Verbrugge, Journal of the Electrochemical Society 157 (2010) A508–A516.
[5] K.E. Aifantis, J.P. Dempsey, Journal of Power Sources 143 (2005) 203–211.
[6] F. Yang, Journal of Power Sources (2010), doi:10.1016/j.jpowsour.2010.1006.1082.
[7] K.D. Kepler, J.T. Vaughey, M.M. Thackeray, Journal of Power Sources 81 (1999) 383–387.
[8] W.H. Pu, X.M. He, J.G. Ren, C.R. Wan, C.Y. Jiang, Electrochimica Acta 50 (2005) 4140–4145.
[9] A.D.W. Todd, R.E. Mar, J.R. Dahn, Journal of the Electrochemical Society 153 (2006) A1998–A2005.
[10] J. Hassoun, S. Panero, P. Simon, P.L. Taberna, B. Scrosati, Advanced Materials 19 (2007) 1632–1635.
[11] L.B. Wang, S. Kitamura, T. Sonoda, K. Obata, S. Tanase, T. Sakai, Journal of the Electrochemical Society 150 (2003) A1346–A1350.

[12] J.J. Zhang, Y.Y. Xia, Journal of the Electrochemical Society 153 (2006) A1466–A1471.
[13] N. Tamura, Y. Kato, A. Mikami, M. Kamino, S. Matsuta, S. Fujitani, Journal of the Electrochemical Society 153 (2006) A1626–A1632.
[14] M. Winter, J.O. Besenhard, Electrochimica Acta 45 (1999) 31–50.
[15] H. Li, L.H. Shi, Q. Wang, L.Q. Chen, X.J. Huang, Solid State Ionics 148 (2002) 247–258.
[16] J. Yang, M. Winter, J.O. Besenhard, Solid State Ionics 90 (1996) 281–287.
[17] S.D. Beattie, T. Hatchard, A. Bonakdarpour, K.C. Hewitt, J.R. Dahn, Journal of the Electroceramical Society 18 (2003) A701–A705.
[18] M. Winter, Z. Phys. Chemie-Int. J. Res. Phys. Chem. Chem. Phys. 223 (2009) 1395–1406.
[19] I.A. Courtney, J.S. Tse, O. Mao, J. Hafner, J.R. Dahn, Physical Review B 58 (1998) 15583–15588.
[20] W. Choi, J.Y. Lee, B.H. Jung, H.S. Lim, Journal of Power Sources 136 (2004) 154–159.
[21] J.W. Osenbach, J.M. DeLucca, B.D. Potteiger, A. Amin, R.L. Shook, F.A. Baiocchi, IEEE Transactions on Electronics Packaging Manufacturing 30 (2007) 23–35.
[22] C.C. Chen, Y. Bisrat, Z.P. Lu, R.E. Schaak, C.G. Chao, D.C. Lagoudas, Nanotechnology 17 (2006) 367–374.
[23] F.Q. Yang, Journal of Physics D: Applied Physics 40 (2007) 4034–4038.
[24] F.Q. Yang, Y. Li, Journal of Applied Physics 104 (2008) 113512.
[25] K.N. Tu, J.C.M. Li, Materials Science and Engineering A: Structural Materials Properties Microstructure and Processing 409 (2005) 131–139.
[26] B.Z. Lee, D.N. Lee, Acta Materialia 46 (1998) 3701–3714.
[27] K.N. Tu, Physical Review B 49 (1994) 2030–2034.
[28] M. Sobiech, M. Wohlschlogel, U. Welzel, E.J. Mittemeijer, W. Hugel, A. Seekamp, W. Liu, G.E. Ice, Applied Physics Letters 94 (2009) 221901.
[29] Y.T. Cheng, A.M. Weiner, C.A. Wong, M.P. Balogh, M.J. Lukitsch, Applied Physics Letters 81 (2002) 3248–3250.
[30] R. Hu, H. Liu, M. Zeng, M. Zhu, International Meeting on Lithium Batteries IMLB, Montreal, Canada, 2010.
[31] C.M. Lopez, J.T. Vaughey, D.W. Dees, Journal of the Electrochemical Society 156 (2009) A726–A729.
[32] C. Brissot, M. Rosso, J.N. Chazalviel, S. Lascaud, Journal of the Electrochemical Society 146 (1999) 4393–4400.
[33] J.M. Tarascon, M. Armand, Nature 414 (2001) 359–367.
[34] F.Q. Yang, J.C.M. Li, Journal of Materials Science: Materials in Electronics 18 (2007) 191–210.
[35] D.E. Newton, The Chemical Elements, Franklin Watts, New York, 1994.